Glomerulotubular disconnection in neonatal mice after relief of partial ureteral obstruction

BA Thornhill[1], MS Forbes[1], ES Marcinko[1] and RL Chevalier[1]

[1]*Department of Pediatrics, University of Virginia, Charlottesville, Virginia, USA*

Ureteropelvic junction obstruction is a common cause of congenital obstructive nephropathy. To study the pathogenesis of nephropathy, a variable-partial, complete or a sham unilateral ureteral obstruction (UUO) was produced in mice within 2 days of birth. The obstruction was released in some animals at 7 days and kidneys harvested at 7–42 days of age for histologic and morphometric study. Renal parenchymal growth was stunted by partial UUO with the impairment proportional to the duration and severity of obstruction. Proximal tubule apoptosis and glomerulotubular disconnection led to nephron loss. Relief of partial UUO arrested glomerulotubular disconnection, resolved tubule atrophy, and interstitial fibrosis with remodeling of the renal architecture. Relief of severe UUO did not result in recovery. Compensatory growth of the contralateral kidney depended on the severity of obstruction. Our studies indicate that relief of moderate UUO will minimize nephron loss. Application of this technique to mutant mice will help develop future therapies to enhance nephron recovery.

Kidney International (2007) **72**, 1103–1112; doi:10.1038/sj.ki.5002512; published online 29 August 2007

KEYWORDS: apoptosis; atubular glomeruli; fibrosis; recovery

Correspondence: *RL Chevalier, Department of Pediatrics, University of Virginia, Box 800386, Charlottesville, Virginia 22908, USA.*
E-mail: RLC2M@virginia.edu

Received 3 April 2007; revised 19 June 2007; accepted 3 July 2007; published online 29 August 2007

Congenital ureteropelvic junction (UPJ) obstruction is the most common cause of obstructive nephropathy in children.[1] The etiology of upper urinary tract abnormalities is poorly understood, but is likely the product of genetic and environmental interactions.[2] To elucidate its pathophysiology, models of partial unilateral ureteral obstruction (UUO) have been developed in the fetal or neonatal sheep, guinea-pig, pig, and rat.[3] Although nephrogenesis is complete before birth in the human, sheep, and guinea pig, it continues postnatally in the pig, rat, and mouse.[3] Spontaneous unilateral or bilateral ureteral obstruction has been reported in strains of rats[4] and mice,[5] but the responsible genetic loci have not been determined. The mouse has the advantage of the availability of numerous targeted mutants, some of which result in a phenotype of spontaneous UPJ obstruction.[6] These suggest that a defect in ureteropelvic smooth muscle development can lead to abnormal ureteral peristalsis and significant functional partial UUO.[7]

Many aspects of the cell biology of obstructive nephropathy have been elucidated recently through the surgical induction of complete UUO in the adult mouse.[8] Studies from our laboratory have described the renal cellular response to complete UUO in a variety of neonatal knockout mice, and have revealed a number of molecules contributing to the response of the developing kidney.[9–12] However, most clinical obstructive nephropathy is attributable to partial, rather than complete, urinary tract obstruction. We have recently described a model of variable chronic partial UUO in the neonatal rat that closely parallels the spectrum of human congenital UPJ obstruction.[13] To take advantage of the many available genetically modified mouse strains, we have developed a model of variable partial UUO in the neonatal mouse. As surgical correction is the only current treatment for significant ureteral obstruction, we have also developed a reproducible means of removing the obstruction to study the cellular process of renal recovery. The results of this approach reveal potentially preventable and reversible alterations in the developing and maturing nephrons of the postobstructed kidney.

RESULTS

As shown in Figure 1, body weight increased approximately fourfold from 7 to 28 days of age, and there were no consistent effects of partial or complete UUO on somatic

growth of the mice. Partial UUO caused progressive hydronephrosis, which was largely prevented by release of obstruction (Figure 2d and e). Figure 3 shows kidney weight for individual mice (including those with partially obstructed ureters not remaining patent, which were not included in histologic analysis). Kidney weight was maintained in 21-day-old mice subjected to 0.2 mm partial UUO with or without relief of obstruction (Figure 3a), but in 28-day-old animals kidney weight was decreased in postobstructed kidneys (Figure 3c). By 28 days of age, kidney weight was lower in the obstructed kidney and greater in the contralateral kidney, with the effect being proportional to the severity of obstruction (Figure 3c and d). By 42 days, kidney weight had decreased in obstructed kidneys and increased in contralateral kidneys, but was normalized by relief of obstruction (Figure 3e and f).

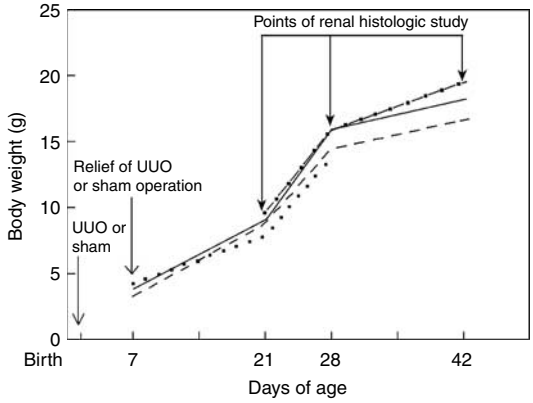

Figure 1 | Experimental design and mean body weight for each of the groups of mice throughout the period of study. There was no overall significant difference in body weight between groups. Partial UUO or sham operation was performed within the first 36 h of life, and in animals undergoing relief of obstruction, this was performed at 7 days of age. Kidneys were removed for study at 7, 14, 21, 28, and 42 days of age. Solid line, sham operation; dashed line, 0.2 mm partial UUO; dash-dotted line, relief of 0.2 mm UUO; dotted line, complete UUO.

Following 14–28 days of 0.2 mm partial UUO, approximately 75% of ureters remained patent, whereas after 42 days of obstruction, more than 50% had become completely occluded (Figure 4a). There was no spontaneous ureteral occlusion in mice undergoing relief of 0.2 mm partial UUO (Figure 4a).

Renal parenchymal thickness increased markedly in sham-operated mice from 14 to 21 days, with little additional increase by 42 days (Figures 2d and 4b). In contrast, renal parenchymal thickness failed to increase regardless of the severity of persistent partial UUO (Figure 4b), and actually decreased with complete UUO (not shown). Following relief of obstruction, renal parenchymal thickness increased (Figures 2d and 4b). At 7 days of age, tubular apoptosis increased following partial or complete UUO (Figure 4c), whereas at 21 days, apoptosis had decreased approximately

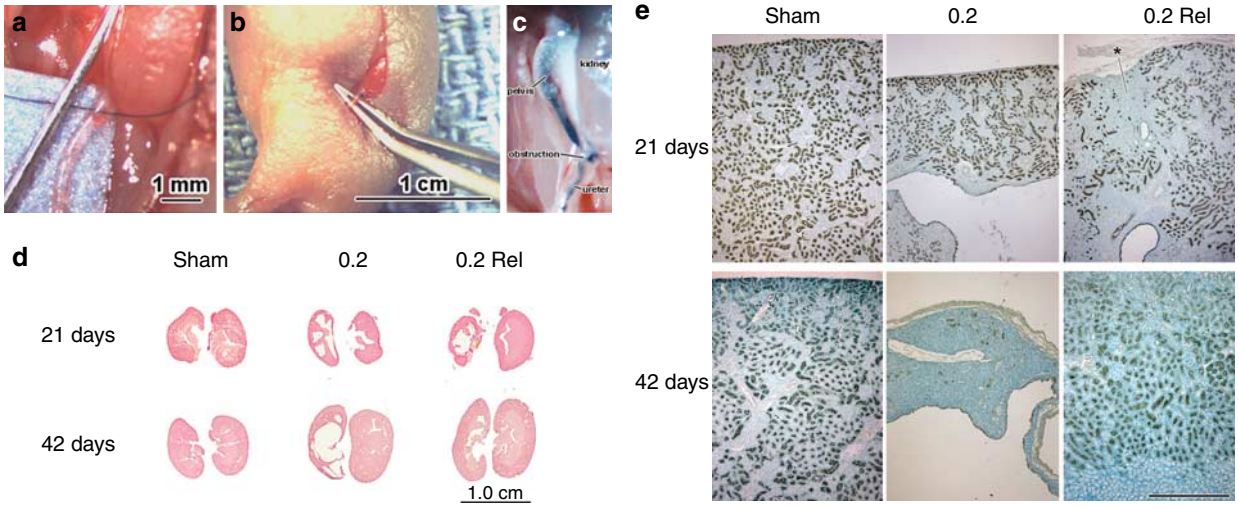

Figure 2 | Surgical technique for creation for partial ureteral obstruction in neonatal mouse, and appearance of kidneys at 21 and 42 days of age. (**a**) A 3–4 mm length of stainless steel wire template was placed adjacent to the ureter, and an 8-0 nylon ligature was tied around both template and ureter at the UPJ. (**b**) The template was removed, leaving the ligature in place just above forceps. (**c**) India ink was injected into the renal pelvis to confirm ureteral patency. (**d**) Sagittal sections from representative obstructed, (left) and contralateral (right) kidneys from sham, 0.2 mm partial UUO, and 0.2 mm partial UUO – relief (Rel) at 21 and 42 days of age. (**e**) Survey micrographs of Lotus-lectin-stained sagittal sections, arranged to correspond to the categories shown in (**d**) (0.2 and 0.2 Rel categories show obstructed-side kidneys). Lotus-lectin staining identifies the complement of proximal convoluted tubules (PCTs). In both 21- and 42-day-old sham-operated animals, PCTs are present in a similar pattern of distribution in the cortex. In the 21-day-old kidney with persistent obstruction (0.2), PCTs appear distributed through the kidney wall, which at this point has lost much of its medullary component. The 21-day postobstructed kidney (0.2 Rel) contains a discrete region in its wall that lacks lectin stain (*); this zone was found on close inspection to contain atubular glomeruli (cf. Figure 6b). In 42-day-old mice with persistent partial UUO, the kidney wall continues to be severely thinned, but contains only scattered PCT remnants and large areas of atubular glomeruli (cf. Figure 7a). The postobstructed kidney at 42 days contains normal-appearing parenchyma (cf. Figure 7b). Bar = 250 μm and applies to all panels in (**e**).

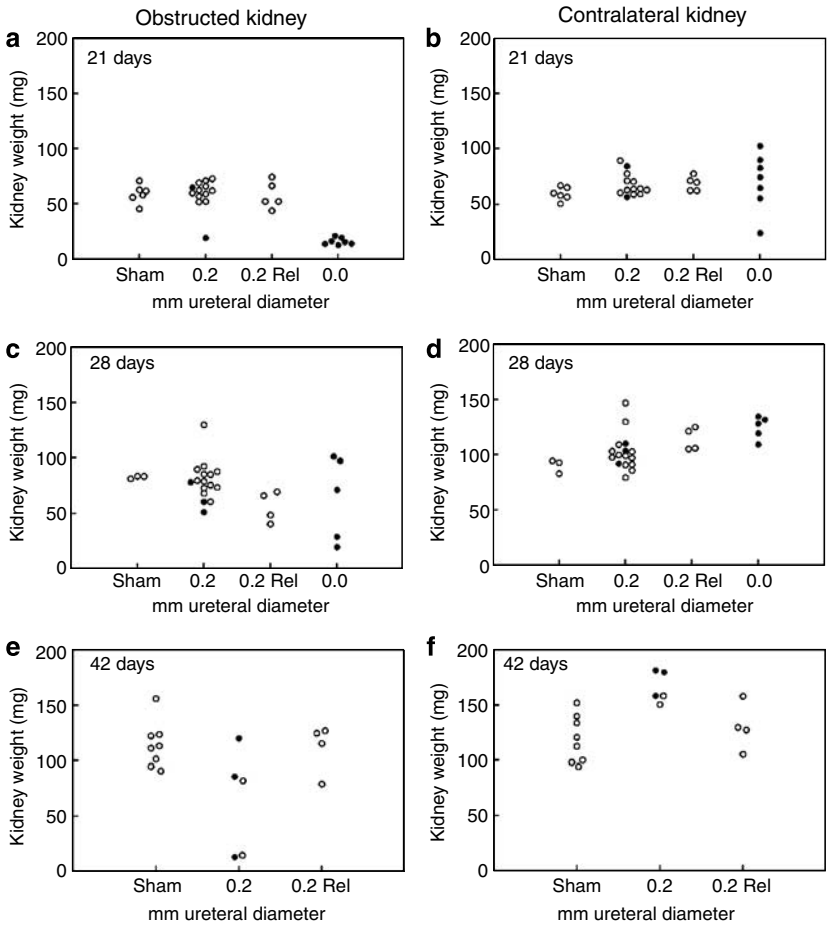

Figure 3 | Relationship of individual kidney weight to the severity of obstruction. (**a**) Twenty-one days, obstructed kidney; (**b**) 21 days, contralateral kidney; (**c**) 28 days, obstructed kidney; kidney weight of mice with 0.2 mm persistent obstruction was greater than that of mice with relief of obstruction (($P<0.05$). (**d**) Twenty-eight days, contralateral kidney. Contralateral kidney weight was greater than that of obstructed kidney for each group ($P<0.05$). (**e**) Forty-two days, obstructed kidney; (**f**) 42 days, contralateral kidney. Contralateral kidney weight of mice with 0.2 mm obstruction was greater than that of sham-operated or postobstructed mice ($P<0.05$). Open circles represent animals with patent left ureters (based on passage of injected India ink past the obstruction); closed circles represent animals with occluded ureters. Only mice with patent ureters were used for histologic study.

10-fold in the persistently obstructed or postobstructed kidney (Figure 4d).

At either 21 or 42 days, the number of glomeruli was not altered by 0.2 mm partial UUO or by its relief (Figure 5a and b). Despite maintenance of patency, relief of 0.1 mm partial UUO did not prevent a decrease in the number of glomeruli at 21 days (99.6 ± 15.2 in the postobstructed vs 163.4 ± 23.1 in the contralateral kidney, $P<0.05$). Although kidney weight and glomerular number were preserved in mice undergoing relief of 0.2 mm partial UUO, tubular atrophy was increased compared with sham-operated mice at 21 days, but was not detectable at 42 days (Figure 5c). In 21-day-old mice recovering from relief of 0.2 mm partial UUO, in contrast to most of the renal parenchyma (Figure 6a and c), there were distinct areas of glomerulotubular disconnection in the postobstructed kidney (Figure 6b and d). This was associated with tubular apoptosis and tubular atrophy (Figure 6e–g), along with pinching off of the tubule from the glomerulus (Figure 6h–m). At 21 days, renal interstitial collagen following relief of 0.2 mm partial UUO remained elevated (Figure 5d).

By 42 days of age, there was further evolution of the lesion in animals with persistent partial UUO compared with those undergoing relief of obstruction (Figure 2e). The renal parenchyma of persistently obstructed kidneys was dominated by clusters of small glomeruli that – on the basis of Lotus-lectin staining – lacked any connection to proximal tubules (Figures 7a, 8a, and b). Proximal tubules had not completely disappeared, however, and could be identified as scattered profiles, thinner and more tortuous than the few normal-appearing tubules remaining in these kidneys (Figure 7c and d). Serial sections of the degenerating profiles confirmed that many of them maintain continuity as tubular structures, but that their lumina were now filled with dense precipitate corresponding to the lectin-specific apical material. Some lectin-positive profiles suggest that the tubules are beginning to undergo fragmentation (Figure 7d). This was associated with ongoing tubular cell death with morphologic characteristics of apoptosis (Figure 7e).

After 42 days, the postobstructed kidneys contained no additional atubular glomeruli, and although their parenchyma

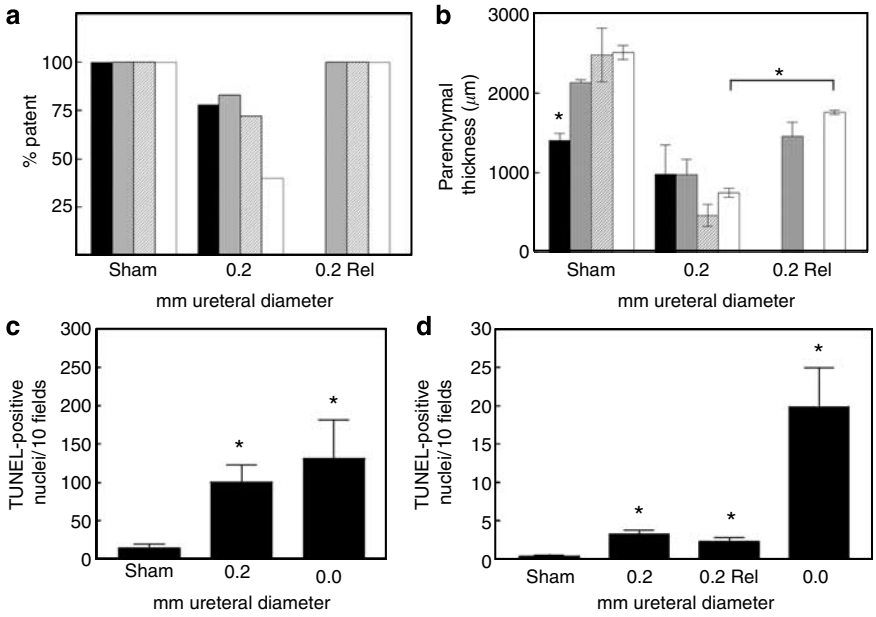

Figure 4 | Effects of partial ureteral obstruction and its release on ureteral patency, renal parenchymal thickness, and renal apoptosis. (**a**) Fraction of ureters remaining patent for sham-operated and partially obstructed ureters at 14 days (black bars), 21 days (cross-hatched bars), 28 days (hatched bars), and 42 days (white bars). (**b**) Mean parenchymal thickness of sham-operated and obstructed kidneys. Same legend as Figure 3a; $^*P<0.05$. (**c**) Density of TUNEL-positive nuclei in the left kidney of 7-day-old mice, expressed as a total of 10 fields. $^*P<0.05$ vs sham. (**d**) Density of TUNEL-positive nuclei in the left kidney of 21-day-old mice. Note scale of ordinate is expanded 10-fold compared to (**c**). $^*P<0.05$ vs sham.

was somewhat thinned (Figure 2e), it consisted of glomeruli of normal size and appearance that remained connected to proximal tubules (Figures 7b, 8a, and b). This parenchyma was nearly indistinguishable in histological appearance from that of the contralateral kidney and the sham-operated kidneys of the same age (Figure 2e). Close examination, however, revealed occasional focal areas of tubular apoptosis and small crowded glomeruli (Figure 7f). In accordance with these observations, tubular atrophy and interstitial fibrosis had decreased and were minimal at this age in the postobstructed kidneys (Figure 5c and d).

DISCUSSION

This study demonstrates in the neonatal mouse that renal growth impairment and cellular injury are dependent on both the severity and the duration of partial ureteral obstruction. Recovery following relief of temporary partial UUO in the neonatal mouse is also dependent on the severity of obstruction: recovery from 0.1 mm (severe) obstruction is poor, with loss of approximately 50% of nephrons by 21 days of age. In contrast, despite significant signs of cellular injury at 21 days, recovery from 0.2 mm (moderate) obstruction improves with time, with remarkable remodeling of renal architecture by 42 days.

As spontaneous occlusion of the partial obstruction can develop with increasing severity and duration of obstruction, selection of an optimal degree of ureteral constriction for future experimental studies will depend on the desired duration of obstruction or recovery. Thus, persistent 0.1 mm partial UUO is too severe, whereas 0.2 mm UUO retains greater than 70% ureteral patency after 28 days. However, patency drops to less than 50% by 42 days, and persistent 0.2 mm UUO would therefore be useful primarily for studies of less than 1-month duration. By 42 days, kidneys with persistent 0.2 mm UUO are severely hydronephrotic with small atubular glomeruli. Relief of 0.1 or 0.2 mm obstruction preserves ureteral patency, however, and would be useful in studying long-term recovery.

The most interesting findings of this study emerge from the renal response to relief of 0.2 mm (moderate) obstruction. Although relief of UUO preserves the number of glomeruli, there is ongoing tubular apoptosis and necrosis within a subset of nephrons, concentrated at their glomerulotubular junctions and leading to the development of tubular atrophy and atubular glomeruli (Figure 8c). Using Lotus-lectin to identify the proximal tubule segments as well as the columnar cells that extend onto the glomerular capsule in serial sections, we have defined criteria for atubular glomeruli in mice. These criteria include (1) small glomerular size, (2) crowding of multiple glomeruli, and (3) lack of Lotus-lectin-positive profiles on Bowman's capsules. On the basis of these criteria, following the relief of 0.2 mm partial UUO, approximately 20% of the glomeruli at 21 days of age are atubular, and there is significant tubular atrophy. Apparent transient worsening of tubular lesions following relief of obstruction has been reported in rats subjected to 2 weeks of UUO.[14] In this study, after an additional 3 weeks of recovery (42 days of age), the postobstructed kidneys show only a few atubular glomeruli and no detectable tubular atrophy, suggesting that most of the atubular glomeruli (and tubular

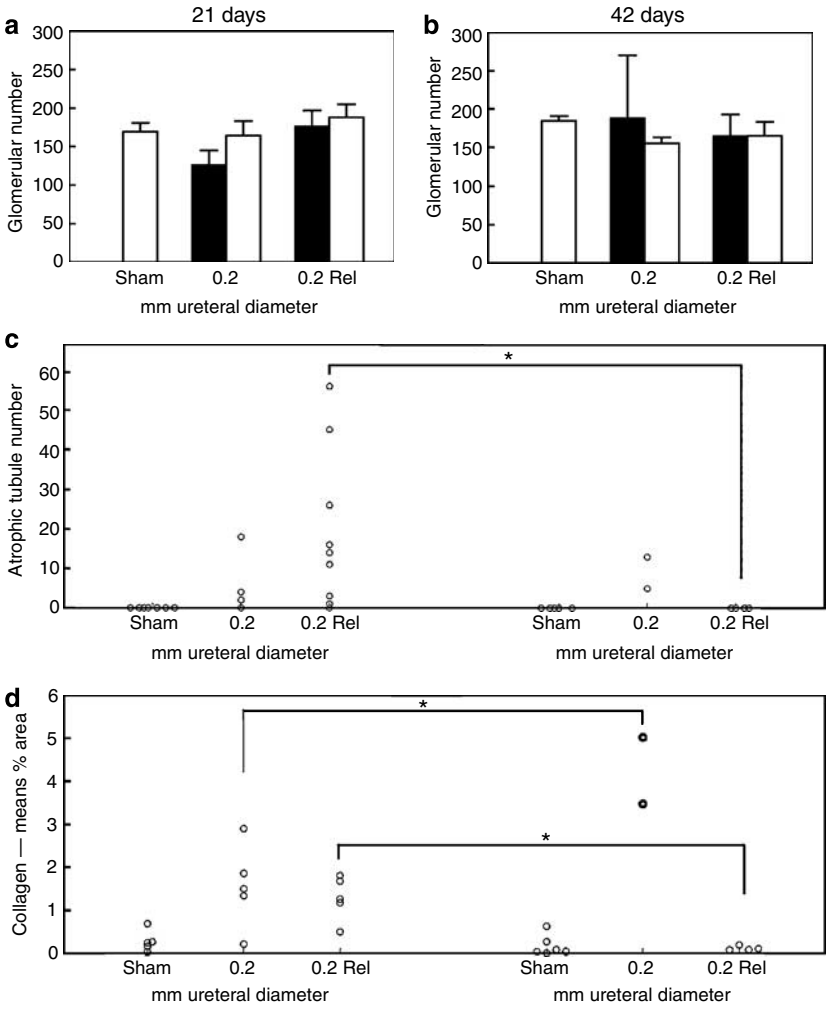

Figure 5 | Renal morphometric results for 21-day-old mice and 42-day-old mice following sham operation or partial UUO with or without release of 5 days' obstruction. (**a**, **b**) Glomerular number. Solid bars, left (obstructed kidney); white bars, right (contralateral kidney); mean ± s.e. (**c**) Relative density of atrophic tubules (left kidney only). Each point represents data from one animal; $^*P < 0.05$ 21 vs 42 days. (**d**) Fractional collagen distribution (left kidney only). Each point represents data from one animal; $^*P < 0.05$ 21 vs 42 days.

fragments) present at 21 days have disappeared. Although the latter would rule against the observed finding of normal numbers of glomeruli in the postobstructed kidney after 42 days, this is likely due to the statistically insignificant reduction in the fraction of tubular glomeruli at 21 days in the postobstructed kidney (Figure 8a), and the error inherent in the calculation of relative glomerular number.

This lesion is similar to the one we recently reported in mice lacking functional endothelial nitric oxide synthase (eNOS).[15] In these animals, kidneys appear normal at birth, but develop focal scars with apoptosis and necrosis at the glomerulotubular junction, resulting in the accumulation of atubular glomeruli in adulthood.[15] Renal expression of eNOS is suppressed by complete UUO in the neonatal rat,[16] and renal eNOS activity is reduced in proportion to the severity of renal interstitial fibrosis in children with UPJ obstruction.[17] Although eNOS is primarily restricted to endothelial cells in the adult kidney, in the neonatal mouse, it is distributed throughout the proximal tubules.[15] If eNOS acts as a survival factor for tubular epithelial cells,[18] ureteral obstruction may favor cell death and glomerulotubular disconnection by downregulating this enzyme.

Similar glomerulotubular disconnection has been described in other experimental renal disorders, including toxic nephropathy,[19–21] ischemic renal injury,[22] renal artery stenosis,[23] and polycystic kidney disease.[24] This phenomenon has also been described in human renal disease: in renal allograft rejection[25] and pyelonephritis.[26] A number of investigators have therefore concluded that glomerulotubular disconnection represents a major mechanism underlying progressive renal disease.[27–29] Such lesions are associated with activation of angiotensin II,[30] and treatment with an angiotensin converting enzyme inhibitor prevents glomerulotubular disconnection in rats with passive Heymann nephritis.[31] Ureteral obstruction markedly activates the renin–angiotensin system, which is already activated in the developing kidney.[32] Although angiotensin inhibition would seem to be an attractive therapeutic approach to congenital

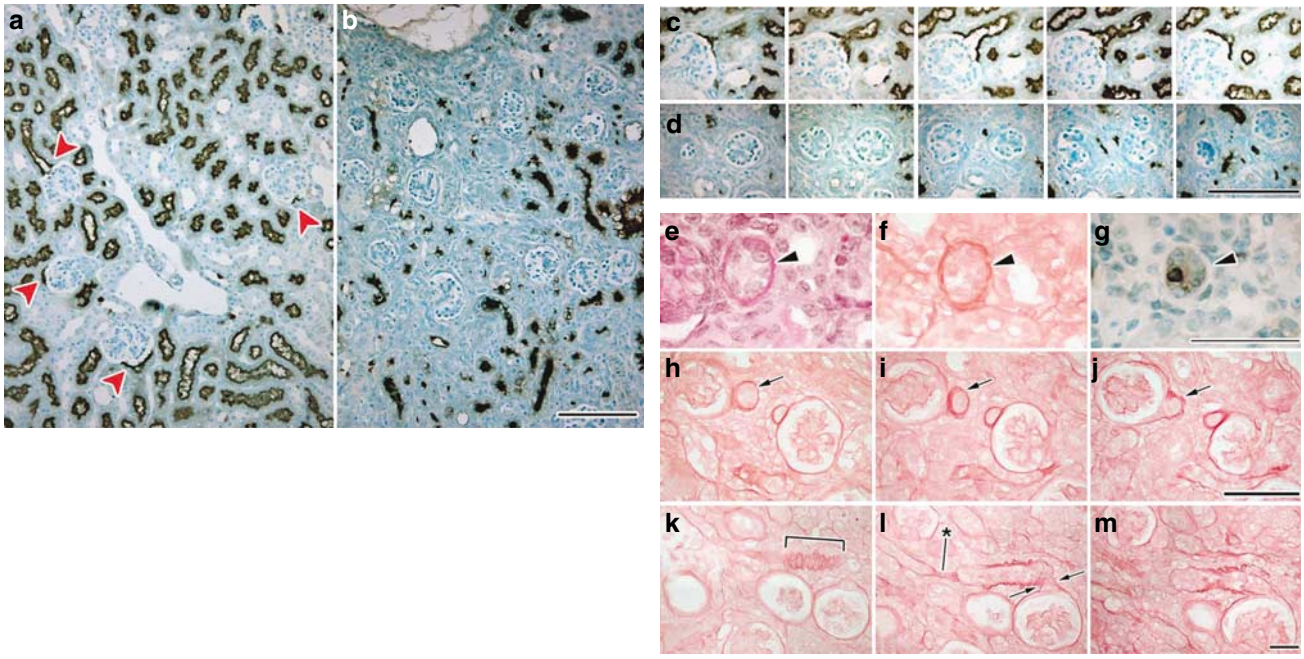

Figure 6 | Kidneys from 21-day-old mice following relief of 5 days of 0.2 mm partial UUO. (**a–d**) Lotus-lectin staining. (**a**) Cortex of the postobstructed kidney. In this region, in addition to staining the lumina of proximal tubules, the biotinylated lectin also attaches to the apices of cells, which extend from the urinary pole around Bowman's capsule (red arrowheads). (**b**) Another region of the same kidney shown in (**a**), in which Bowman's capsules lack any lectin staining. (**c** and **d**) Serial-section arrays: (**c**) Consecutive sections of a glomerulus showing continuity of the lectin-stained cells of Bowman's capsule with the proximal tubule (lectin positivity is present within the glomerulus in all sections). (**d**) Zone in the postobstructed kidney similar to that shown in (**b**). Although lectin-positive profiles appear in the region, none of them are connected to the glomeruli, which are smaller than their lectin-positive counterparts in (**c**), indicating that such glomeruli are atubular. (**e–g**) Serial consecutive sections showing periodic-acid Schiff staining, picrosirius red staining, and TUNEL reaction for apoptosis, respectively. The arrowhead is placed at the outer margin of thickened tubular basement membrane, which shows that periodic-acid Schiff and Sirius red reveal identical staining and contours, whereas in (**g**), the tubular basement membrane fails to stain with methylene blue counterstaining (note apoptotic nucleus in the atrophied tubule wall). (**h–j**) Consecutive serial sections of picrosirius-stained postobstructed kidneys. In (**h** and **i**), characteristic atrophic tubule profiles (arrows) are closely apposed to glomeruli. In (**j**), the tubule marked by the arrow is continuous with Bowman's capsule, indicating that it is a proximal tubule segment. (**k–m**) Another series of consecutive sections, focusing on a glomerulus (lower right of panels) and its proximal tubule. (**k**) A tangential section of the tubular basement membrane to be pleated and thickened (bracket). In (**l**), the proximal tubule segment at its junction with the glomerulus is pinched at an acute angle (between arrows), and the rugose tubular basement membrane profile is evident in longitudinal section, along with a severely narrowed segment to the left (*). Bar in (**b**) equals 100 μm and applies to both (**a**) and (**b**); bar in (**d**) equals 100 μm and applies to all 10 panels in (**c**) and (**d**); bar in (**g**) applies to (**e–g**) and equals 50 μm; bar in (**j**) applies to (**h–j**) and equals 50 μm; bar in (**m**) applies to panels (**k–m**) and equals 20 μm.

obstructive nephropathy, caution must be exercised, because angiotensin is necessary for normal renal development and maturation, and its inhibition can in fact exacerbate renal injury resulting from partial UUO.[33]

Although glomerulotubular disconnection may represent a major pathway for nephron loss resulting from UUO in the neonatal mouse, alternative mechanisms may predominate in other species. In the neonatal rat subjected to partial UUO, 50% of recognizable glomeruli disappear by 28 days, possibly as a result of cellular phenotypic transformation.[13] In contrast, 1 year following the relief of temporary complete UUO in the neonatal rat, glomeruli undergo progressive sclerosis.[34] Chronic partial UUO in the neonatal rat also results in apoptosis, tubular atrophy, and interstitial fibrosis proportional to the severity of obstruction.[13] Kidneys from infants with UPJ obstruction reveal glomerular changes as well as altered dimensions of renal tubules.[35] In patients over 1 year of age, renal interstitial fibrosis is more common,[35] and presumably reflects progression of the injury over time. Kidneys from children with severe UPJ obstruction contain sclerotic glomeruli, atrophic tubules, and interstitial fibrosis, changes that are similar to those that develop in rodent models.[36,37] In children undergoing pyeloplasty for UPJ obstruction, although renal function improved in all but one patient, 14 of 33 patients had persistently abnormal renal function.[38] Renal function increased significantly in children undergoing operation under 1 year of age, but normalized in only one of six patients over 1 year old.[38] In 343 children with antenatal diagnosis of UPJ obstruction initially managed by observation alone, over 50% ultimately required surgical correction.[39] Similarly, early relief of partial UUO in neonatal rats allows recovery of normal function, whereas later relief of obstruction does not.[40] These studies suggest that earlier surgical intervention is more effective, and that residual renal injury limits ultimate renal recovery.

Equally remarkable is the finding in this study that by 42 days, most atrophic tubular remnants have been cleared and interstitial fibrosis has regressed completely (Figure 5c and d).

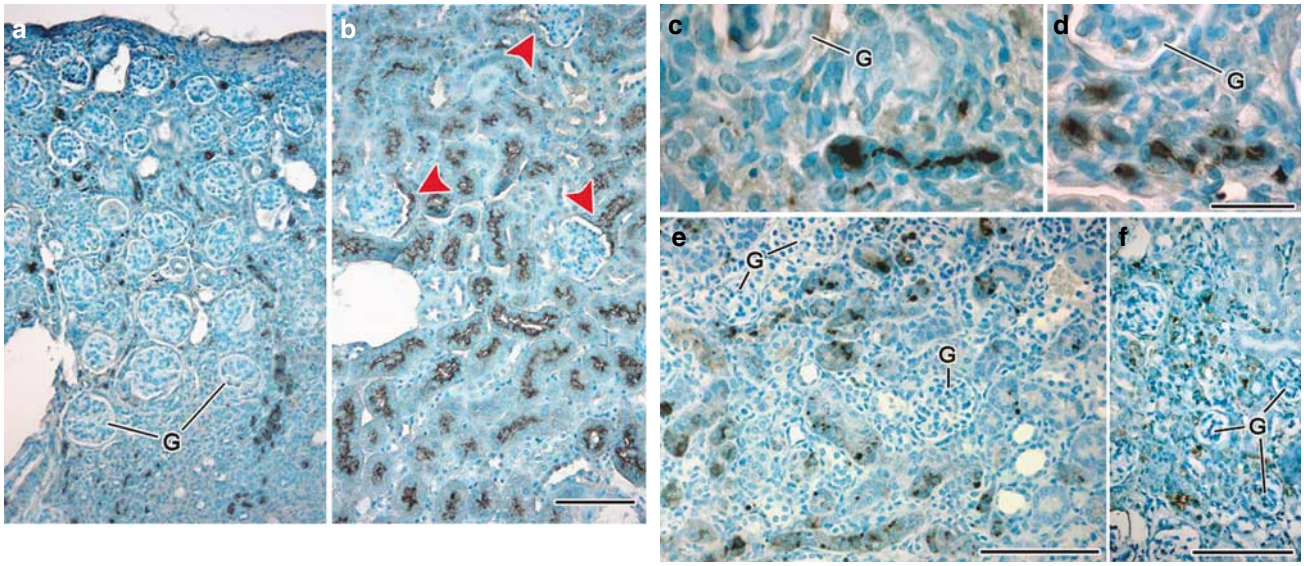

Figure 7 | Forty-two-day-old mouse kidney comparing persistent UUO with release of obstruction. (**a**) Kidney from mouse with persistent ipsilateral 0.2 mm partial UUO; this kidney still exhibited ureteral patency at the time of killing, but showed a high degree of hydronephrosis (cf. Figure 1d) with substantial thinning of the kidney wall. A striking feature of the remaining parenchyma is the presence of numerous clustered glomeruli, none of which in this Lotus-lectin-stained preparation display any connection with proximal tubules. The lectin-stained profiles in the general vicinity of the glomerular clusters correspond to proximal tubule remnants that have become separated from their parent glomeruli (G). (**b**) Equivalent view of cortex from Lotus-stained section of a kidney undergoing relief of obstruction after 5 days of 0.2 mm partial UUO and harvested at 42 days of age. Although this kidney was slightly hydronephrotic (cf. Figure 2d), its parenchyma exhibits a uniformly normal appearance, with normally distributed glomeruli that either bear the typical 'crescent' of lectin staining or can be seen to be in direct connection with proximal tubules (arrowheads). (**c** and **d**) High magnification details from the persistently obstructed kidney shown in (**a**). (**c**) An atrophic proximal tubule is distorted with a tortuous lumen of varying bore and an atubular glomerulus (G). (**d**) Proximal tubule remnants are present near an atubular glomerulus (G) and densely staining material fills their luminal cavities, indicating that the tubules have shrunken and have undergone fragmentation. (**e**) Kidney from 42-day-old 0.2 mm persistently obstructed mouse, TUNEL-stained. Tubular profiles whose walls are composed largely of apoptotic cells are scattered among atubular glomeruli (G). (**f**) Kidney from 42-day-old 0.2 mm postobstructed mouse. This small pocket of TUNEL-positive cells and atubular glomeruli (G) was the only histologically abnormal region found in this kidney. Bar in (**b**) equals 100 μm and applies to both (**a**) and (**b**). Bar in (**d**) equals 25 μm and applies to both (**c**) and (**d**). Bars in (**e**) and (**f**) equal 100 μm for their respective panel.

This is a dramatic example of the plasticity of renal cells, and their role in remodeling.[41] In this regard, 6 weeks of recovery following relief of 10 days of complete UUO in the adult mouse leads to significant recovery of proximal tubular lesions.[42] Reversal of glomerular and interstitial fibrosis is an area of active investigation, and the present model should prove useful in finding new therapeutic approaches to accelerate the removal of matrix material.[43,44] However, following prolonged partial UUO, renal recovery in the neonatal rat is poor, suggesting that for optimum recovery, severe obstruction should be released soon after the completion of nephrogenesis.[40] The molecular basis for age-dependent differences in the renal response to obstruction is only beginning to be understood. In a preliminary report of complete UUO in neonatal and adult mice, there was marked early upregulation of Gdnf and Six2 in both obstructed and contralateral neonatal kidneys, but there was delayed upregulation in adult obstructed kidneys, and a much weaker response by the adult contralateral kidney (Lange-Sperandio, *J Am Soc Nephrol* 2006; **17**:444A).

In this study, the compensatory growth response of the neonatal mouse kidney was significant after 21–28 days of contralateral partial UUO. This contrasts with the more delayed response in the neonatal rat kidney.[45] Moreover, relief of obstruction prevented compensatory growth of the contralateral kidney by 42 days (Figure 3e and f). Thus, compensatory growth of the contralateral kidney reflects the degree of impairment of the obstructed kidney, an observation that in the past led to the proposal that contralateral renal growth could serve as an index of the severity of obstruction.[46]

In conclusion, we describe a new model of reversible, variable partial UUO in the neonatal mouse. Renal growth is impaired in relation to the duration and severity of obstruction, and is restored by relief of the obstruction. Compensatory growth of the contralateral kidney is dependent on the degree of impairment of the obstructed kidney. As a result of partial UUO, tubules undergo progressive apoptosis and necrosis, by 42 days generating a population of small glomeruli that are atubular and thus nonfunctional. In contrast, relief of the obstruction after 5–6 days of partial UUO limits the fraction of atubular glomeruli to only 20% by 21 days, and by 42 days, the kidney has undergone extensive remodeling. This model should prove useful in the study of pathophysiology of congenital obstructive nephropathy, and in the development of interventions to improve or prevent its progression.

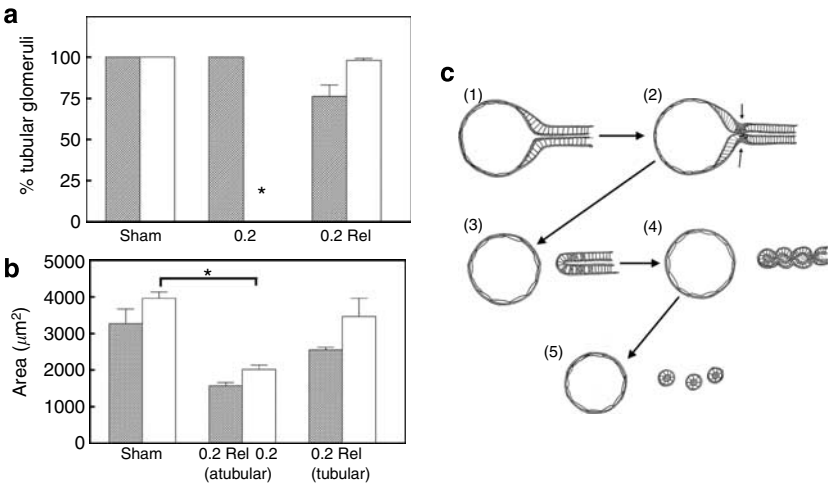

Figure 8 | Distribution and size of atubular glomeruli, and proposed scheme of process of glomerulotubular disconnection. (**a** and **b**) Distribution and sizes of tubular and atubular glomeruli in 21-day-old (solid bars) and 42-day-old kidneys (open bars). (**a**) Percentage of glomerular populations that consists of tubular glomeruli (i.e., still connected to proximal tubules). Although at 21 days all glomeruli in kidneys with persistent obstruction retain their tubular connections, by 42 days, no tubule-connected glomeruli remained in the kidneys examined, although ureters remained patent. In contrast, in post-obstructed kidneys at 21 days, approximately 20% of all glomeruli are atubular, but after 42 days, virtually all remaining glomeruli are tubular. *$P<0.05$ vs 21-day-old. (**b**) Areas of the glomeruli compared between kidneys of 21- and 42-day-old mice, showing the small size of atubular glomeruli compared with their tubule-connected counterparts. *$P<0.05$. (**c**) Steps in 'detubulation,' the separation of the glomerulus from its proximal tubule. Glomerular tuft is omitted for clarity in this diagram. (1) In the mouse glomerulus, tall epithelial cells make up part of Bowman's capsule, blending into the proximal convoluted tubules (PCT) and bearing on their apical surfaces the same Lotus-lectin affinity that characterizes the PCT epithelial cells. (2) Apoptotic nuclei appear in the neck region where the PCT emerges from the glomerulus, leading there to thickening of the basement membrane (between small arrows) and marked thinning of the tubule diameter. (3) The PCT becomes disconnected from the glomerulus, which loses all Lotus-lectin positivity. The severed PCT begins to undergo degeneration through a combination of epithelial cell apoptosis and necrosis. (4) Although the glomerulus remains intact, the disconnected tubule continues to degenerate, maintaining luminal lectin positivity but assuming an irregular shrunken profile. (5) Eventually, the PCT breaks into spherical fragments, each of which retains a lectin-positive core. The atubular glomerulus persists for an indeterminate time, although it may undergo ultimate resorption.

MATERIALS AND METHODS

Animal surgery

Breeding pairs of C57/BL5 mice (Charles River Laboratories, Wilmington, MA, USA) were maintained in the University vivarium, and pups were weaned at 21 days of age. Mice were subjected to UUO or sham operation 24–48 h following birth. The timing of obstruction is critical, as nephrogenesis progresses rapidly in the postnatal mouse, with new nephron induction ending on postnatal day 3, when new nephrons form *en masse* (Hartman and Patterson, *J Am Soc Nephrol* 2005; **16**: 578A). We wished to create the obstruction during active nephrogenesis, so as to parallel the development of human UPJ obstruction. At the time of operation, mice were removed from their mothers and anesthetized with isoflurane and oxygen. All surgery was performed using sterile technique in accordance with a University of Virginia Animal Care and Use Committee approved animal protocol. The left ureter was exposed through a flank incision and a 3–4 mm length of stainless steel wire (T-304V) (Small Parts Inc., Miami, FL, USA) was placed adjacent to the ureter (Figure 2a). An 8-0 nylon ligature was tied around both ureter and template at the UPJ, and the template was removed (Figure 2b). In preliminary studies, wire diameters of 0.3, 0.2, and 0.1 mm were used: 0.3 mm created mild obstruction; 0.2 mm moderate obstruction; and 0.1 mm severe obstruction. All kidneys with 0.3 mm obstruction ($n=6$) maintained ureteral patency through 28 days, whereas only 33% of those with 0.1 mm obstruction ($n=12$) were patent at 28 days. To characterize the model in more detail, this study focuses on animals with 0.2 mm obstruction ($n=52$), and compares them with sham operation ($n=21$) and complete UUO ($n=12$). Sham-operated pups underwent the same procedure, except that the ureter was left intact, and pups in the 0.0 mm (complete UUO) groups had their ureters completely ligated. The incision was closed with 8-0 polypropylene suture and sealed with tissue cement. Animals recovered, and then were returned to their mothers.

Under sterile technique conditions, a second operation was performed on day 7 of age (after 5–6 days of partial UUO or sham operation). A 3–5 mm incision was made parallel to and approximately 2 mm to the left of the mid-line. The ureter and its ligature were exposed. Under $\times 20$ magnification, the knot was teased free of surrounding tissue, cut with superfine Vannas scissors (Fine Science Tools, Foster City, CA, USA), and was removed with Dumont no. 5CO forceps (Fine Science Tools). Animals with persistent UUO and sham-operated mice underwent the same manipulation, but the ligature was left intact. Pups were allowed to recover and were returned to their mothers. Sutures were removed 5–7 days following each operation.

Tissue harvest

At 7, 14, 21, 28, or 42 days of age, animals were weighed and then killed with Euthanol solution. India ink was injected into the pelvis to establish patency (Figure 2c). Only kidneys with patent ureters were included in the histologic studies. Kidneys were removed to ice-cold saline; in selected animals, the capsules were removed and the kidneys were weighed. In the remaining kidneys, capsules were left intact with the ureter attached. Kidneys were fixed either by immersion or perfusion with 10% formalin in phosphate buffer.

Tissue preparation

Tissues were embedded in paraffin and cut at 4 μm thickness. Digital micrographs were taken with a Q-Imaging MicroPublisher camera mounted either on a Leica MZ6 operating microscope or a Leica DMLS compound light microscope.

Morphometry

Median sagittal sections of kidneys were stained with picrosirius red as an indicator of fibrosis. These sections were used to generate data for a number of different parameters: (1) Collagen distribution was evaluated by examining 10 non-overlapping fields that sampled the entire section at $\times 400$ total magnification, by means of image-analysis software (Image-Pro® Plus, version 5.1, Media Cybernetics, Silver Spring, MD, USA) and the results expressed as a percent of total area occupied by positive-staining connective tissue. (2) Glomerular numbers were manually counted in each median sagittal section.[47] This indirect measurement of glomerular number has previously been validated using the disector technique for neonatal mice,[48] and we have validated the technique also in the neonatal rat.[49] (3) Renal parenchymal thickness was also measured with the Image-Pro program, but at $\times 40$ total magnification, with three radial measurements made (both poles and opposite the hilum). Detailed examination of sections at higher magnification was made to ensure that the papilla was excluded in making these measurements, as in the sham or contralateral kidney, it would contribute inordinately to the measurement taken opposite the hilum, and also because of its varying degree of retraction during the development of hydronephrosis. Glomerular size, glomerulotubular neck morphology, and tubular atrophy were determined as described previously.[15] Tubular atrophy was quantified for each animal category in the same median sagittal sections used to measure glomerular numbers and capsule thickness. Atrophic tubules were identified as having a markedly thickened, Sirius red-positive tubular basement membrane, and this was confirmed in some cases by periodic-acid Schiff staining of serial consecutive sections.

Lotus-lectin staining

Kidney sections were stained with biotinylated lectin for identification and morphometric evaluation of proximal tubules. Although Lotus tetragonolobus lectin (Vector Laboratories, Burlingame, CA, USA) consistently stains proximal tubules,[50] there is also staining of intercalated cells in cortical collecting ducts, and collecting duct cells of the papilla are strongly stained. However, staining in cortex is concentrated on the luminal coatings of the proximal tubules, allowing their unequivocal identification.

Lectin staining highlights a peculiar feature of mouse glomeruli: at the urinary pole, approximately one-third or more of the epithelial cells constituting Bowman's capsule is made up of cuboidal epithelial cells, continuous with those of the proximal tubule.[51] In addition to resembling proximal tubular epithelium, these cells have similar lectin positivity on their apical surfaces. This can be used as a marker for glomeruli that are attached to intact proximal tubules. Consecutive serial sections of Lotus-lectin-stained kidneys were therefore used to make positive identification of atubular glomeruli.

Apoptosis

Apoptotic nuclei were identified by the terminal deoxy transferase uridine triphosphate nick-end labeling (TUNEL) technique (Apoptag® *In Situ* Detection Kit, Chemicon Inc., Temecula, CA, USA). The relative contribution of these immunostaining cells was quantified as described previously.[52] This staining method can be used to identify both apoptotic cells and cells undergoing necrosis.[15]

Statistical analysis

Comparisons between groups at each age were made by one-way analysis of variance followed by Holm–Sidak multiple comparisons for normally distributed data, and by Kruskal–Wallis one-way analysis of variance followed by Dunn's multiple comparisons for data not normally distributed. Comparisons between 21- and 42-day ages were made by Student's *t*-test for unpaired normally distributed data, and by Mann–Whitney rank sum test for data not normally distributed. Comparisons between left and right kidneys were made using Student's *t*-test for paired data. Statistical significance was defined as $P < 0.05$.

ACKNOWLEDGMENTS

Parts of this work have been published as abstract (Thornhill BA. *J Am Soc Nephrol* 2005; **16**: 222A) and presented at the American Society of Nephrology, Philadelphia, PA, USA, November 2005. This work was supported by grants from the National Institutes of Health, DK52612, DK45179, and DK62328.

REFERENCES

1. Flashner SC. Ureteropelvic Junction. In: Kelalis PP, King LR, Belman AB (eds). *Clinical Pediatric Urology*. Saunders: Philadelphia, 1992, pp 693–725.
2. Woolf AS. A molecular and genetic view of human renal and urinary tract malformations. *Kidney Int* 2000; **58**: 500–512.
3. Matsell DG, Tarantal AF. Experimental models of fetal obstructive nephropathy. *Pediatr Nephrol* 2002; **17**: 470–476.
4. Heuser M, Seseke F, Zoller G *et al.* Differences in cortical microcirculation in the kidneys of unilaterally congenital hydronephrotic rats. *Microvasc Res* 2001; **62**: 172–178.
5. Horton Jr CE, Davisson MT, Jacobs JB *et al.* Congenital progressive hydronephrosis in mice: a new recessive mutation. *J Urol* 1988; **140**: 1310–1315.
6. Chang CP, McDill BW, Neilson JR *et al.* Calcineurin is required in urinary tract mesenchyme for the development of the pyeloureteral peristaltic machinery. *J Clin Invest* 2004; **113**: 1051–1058.
7. Mendelsohn C. Functional obstruction: the renal pelvis rules. *J Clin Invest* 2004; **113**: 957–959.
8. Chevalier RL. Obstructive nephropathy: towards biomarker discovery and gene therapy. *Nat Clin Prac Nephrol* 2006; **2**: 157–168.
9. Fern RJ, Yesko CM, Thornhill BA *et al.* Reduced angiotensinogen expression attenuates renal interstitial fibrosis in obstructive nephropathy in mice. *J Clin Invest* 1999; **103**: 39–46.
10. Lange-Sperandio B, Cachat F, Thornhill BA *et al.* Selectins mediate macrophage infiltration in obstructive nephropathy in newborn mice. *Kidney Int* 2002; **61**: 516–524.
11. Lange-Sperandio B, Schimpgen K, Rodenbeck B *et al.* Distinct roles of Mac-1 and its counter-receptors in neonatal obstructive nephropathy. *Kidney Int* 2006; **69**: 81–88.
12. Yoo KH, Thornhill BA, Forbes MS *et al.* Osteopontin regulates renal apoptosis and interstitial fibrosis in neonatal chronic unilateral ureteral obstruction. *Kidney Int* 2006; **70**: 1735–1741.
13. Thornhill BA, Burt LA, Chen C *et al.* Variable chronic partial ureteral obstruction in the neonatal rat: a new model of ureteropelvic junction obstruction. *Kidney Int* 2005; **67**: 42–52.
14. Yokoyama M, Yoshioka S, Iwata H *et al.* Paradoxical tubular obstruction after release of ureteral obstruction in rat kidney. *J Urol* 1984; **132**: 388–391.
15. Forbes MS, Thornhill BA, Park MH *et al.* Lack of endothelial nitric-oxide synthase leads to progressive focal renal injury. *Am J Pathol* 2007; **170**: 87–99.
16. Silverstein DM, Travis BR, Thornhill BA *et al.* Altered expression of immune modulator and structural genes in neonatal unilateral ureteral obstruction. *Kidney Int* 2003; **64**: 25–35.
17. Valles P, Pascual L, Manucha W *et al.* Role of endogenous nitric oxide in unilateral ureteropelvic junction obstruction in children. *Kidney Int* 2003; **63**: 1104–1115.

18. Tong X, Li H. eNOS protects prostate cancer cells from TRAIL-induced apoptosis. *Cancer Lett* 2004; **210**: 63–71.
19. Marcussen N, Ottosen PD, Christensen S *et al.* Atubular glomeruli in lithium-induced chronic nephropathy in rats. *Lab Invest* 1989; **61**: 295–302.
20. Marcussen N. Atubular glomeruli in cisplatin-induced chronic interstitial nephropathy. *APMIS* 1990; **98**: 1087–1097.
21. Javaid B, Olson JL, Meyer TW. Glomerular injury and tubular loss in adriamycin nephrosis. *J Am Soc Nephrol* 2001; **12**: 1391–1400.
22. Pagtalunan ME, Olson JL, Tilney NL *et al.* Late consequences of acute ischemic injury to a solitary kidney. *J Am Soc Nephrol* 1999; **10**: 366–373.
23. Marcussen N. Atubular glomeruli in renal artery stenosis. *Lab Invest* 1991; **65**: 558–565.
24. Tanner GA, Tielker MA, Connors BA *et al.* Atubular glomeruli in a rat model of polycystic kidney disease. *Kidney Int* 2002; **62**: 1947–1957.
25. Pagtalunan ME, Oberbauer R, Haas M *et al.* Atubular glomeruli in patients with chronic allograft rejection. *Transplantation* 1996; **61**: 1166–1171.
26. Marcussen N, Olsen TS. Atubular glomeruli in patients with chronic pyelonephritis. *Lab Invest* 1990; **62**: 467–473.
27. Marcussen N. Tubulointerstitial damage leads to atubular glomeruli: significance and possible role in progression. *Nephrol Dial Transplant* 2000; **15**(Suppl 6): 74–75.
28. Gibson IW, Downie TT, More IAR *et al.* Atubular glomeruli and glomerular cysts – a possible pathway for nephron loss in the human kidney? *J Pathol* 1996; **179**: 421–426.
29. Kriz W, LeHir M. Pathways to nephron loss starting from glomerular diseases – insights from animal models. *Kidney Int* 2005; **67**: 404–419.
30. Pagtalunan ME, Olson JL, Meyer TW. Contribution of angiotensin II to late renal injury after acute ischemia. *J Am Soc Nephrol* 2000; **11**: 1278–1286.
31. Benigni A, Gagliardini E, Remuzzi A *et al.* Angiotensin-converting enzyme inhibition prevents glomerular-tubule disconnection and atrophy in passive Heymann nephritis, an effect not observed with a calcium antagonist. *Am J Pathol* 2001; **159**: 1743–1750.
32. Chevalier RL, Cachat F. Role of angiotensin II in chronic ureteral obstruction. In: Wolf G (ed). *The Renin-Angiotensin System and Progression of Renal Diseases*, 1st edn Karger: Basel, 2001, pp 250–260.
33. Chen CO, Park MH, Forbes MS *et al.* Angiotensin converting enzyme inhibition aggravates renal interstitial injury resulting from partial unilateral ureteral obstruction in the neonatal rat. *Am J Physiol Renal Physiol* 2007; **292**: F946–F955.
34. Chevalier RL, Thornhill BA, Chang AY. Unilateral ureteral obstruction in neonatal rats leads to renal insufficiency in adulthood. *Kidney Int* 2000; **58**: 1987–1995.
35. Huang WY, Peters CA, Zurakowski D *et al.* Renal biopsy in congenital ureteropelvic junction obstruction: evidence for parenchymal maldevelopment. *Kidney Int* 2006; **69**: 137–143.
36. Elder JS, Stansbrey R, Dahms BB *et al.* Renal histological changes secondary to ureteropelvic junction obstruction. *J Urol* 1995; **154**: 719–722.
37. Stock JA, Krous HF, Heffernan J *et al.* Correlation of renal biopsy and radionuclide renal scan differential function in patients with unilateral ureteropelvic junction obstruction. *J Urol* 1995; **154**: 716–718.
38. Boubaker A, Prior JO, Meyrat B *et al.* Unilateral ureteropelvic junction obstruction in children: long-term follow-up after unilateral pyeloplasty. *J Urol* 2003; **170**: 575–579.
39. Chertin B, Pollack A, Koulikov D *et al.* Conservative treatment of ureteropelvic junction obstruction in children with antenatal diagnosis of hydronephrosis: lessons learned after 16 years of follow-up. *Eur Urol* 2006; **49**: 734–739.
40. Shi Y, Pedersen M, Li C *et al.* Early release of neonatal ureteral obstruction preserves renal function. *Am J Physiol* 2004; **286**: F1087–F1099.
41. El Nahas AM. Plasticity of kidney cells: role in kidney remodeling and scarring. *Kidney Int* 2003; **64**: 1553–1563.
42. Cochrane AL, Kett MM, Samuel CS *et al.* Renal structural and functional repair in a mouse model of reversal of ureteral obstruction. *J Am Soc Nephrol* 2005; **16**: 3623–3630.
43. Fogo AB. Can glomerulosclerosis be reversed? *Nat Clin Prac Nephrol* 2006; **2**: 290–291.
44. Eddy AA. Can renal fibrosis be reversed? *Pediatr Nephrol* 2005; **20**: 1369–1375.
45. Yoo KH, Thornhill BA, Forbes MS *et al.* Compensatory renal growth due to neonatal ureteral obstruction: Implications for clinical studies. *Pediatr Nephrol* 2006; **21**: 368–375.
46. Koff SA, Peller PA, Young DC *et al.* The assessment of obstruction in the newborn with unilateral hydronephrosis by measuring the size of the opposite kidney. *J Urol* 1994; **152**: 596–599.
47. Chevalier RL, Kim A, Thornhill BA *et al.* Recovery following relief of unilateral ureteral obstruction in the neonatal rat. *Kidney Int* 1999; **55**: 793–807.
48. Dziarmaga A, Eccles M, Goodyer P. Suppression of ureteric bud apoptosis rescues nephron endowment and adult renal function in Pax2 mutant mice. *J Am Soc Nephrol* 2006; **17**: 1568–1575.
49. Chevalier RL, Thornhill BA, Chang AY *et al.* Recovery from release of ureteral obstruction in the rat: relationship to nephrogenesis. *Kidney Int* 2002; **61**: 2033–2043.
50. Cachat F, Lange-Sperandio B, Chang AY *et al.* Ureteral obstruction in neonatal mice elicits segment-specific tubular cell responses leading to nephron loss. *Kidney Int* 2003; **63**: 564–575.
51. Zhai XY, Birn H, Jensen KB *et al.* Digital three-dimensional reconstruction and ultrastructure of the mouse proximal tubule. *J Am Soc Nephrol* 2003; **14**: 611–619.
52. Chevalier RL, Goyal S, Wolstenholme JT *et al.* Obstructive nephropathy in the neonatal rat is attenuated by epidermal growth factor. *Kidney Int* 1998; **54**: 38–47.